

Experimental, Statistical and Stochastic Studies of Pressure Fluctuations in a Three-phase Fluidized Bed with a Moderately Large Diameter

Soung Hee Park[†] and Sang Done Kim*

Department of Chemical Engineering, Woosuk University, Chonbuk 565-701, Korea

*Department of Chemical Engineering, Korea Advanced Institute of Science and Technology, Daejeon 305-701, Korea

(Received 26 April 2002 • accepted 27 August 2002)

Abstract—Hydrodynamic properties of bubbling flow through a three-phase fluidized bed with a moderately large diameter have been characterized with statistical and stochastic analyses of a comprehensive set of experimentally measured pressure fluctuations in the bed. The analyses have yielded the fluctuations' histogram, mean, maximum, minimum, standard deviation, skewness, kurtosis, and power-spectral-density function. As the gas flow rate increased with other operating conditions fixed, the mean and standard deviation increased, the skewness decreased, the distribution of the power-spectral-density function broadened, and the major frequency increased. In contrast, as the liquid flow rate increased, the mean and standard deviation decreased, the skewness and kurtosis increased, the power-spectral-density function narrowed, and the major frequency decreased. The hydrodynamic properties of a three-phase fluidized bed with a moderately large column in terms of pressure fluctuations are strongly affected by the flow rates of both the fluidizing gas and liquid.

Key words: Pressure Fluctuations, Fluidized Bed, Statistical Analysis, Stochastic Analysis

INTRODUCTION

Three-phase fluidized beds are ubiquitous in chemical and allied industries and also in pollution control. Often, such a bed comprises the fluidizing-gas bubbles, fluidizing liquid, and fluidized-solid particles, of which the first and third exist as dispersed phases, and the second, as a continuous phase. With its increasing applications to biochemical as well as chemical and petrochemical processes, three-phase fluidization has become one of the most important modes of multiphase contacting. Various attempts have been made to develop reactors and contactors by taking advantage of the unique features of three-phase fluidized beds, such as high contacting efficiency among different phases in terms of the heat and mass transfer rates and low pressure drop [Epstein, 1981; Shah et al., 1982; Fan, 1989].

Judicious design and effective operation of three-phase fluidized beds as contactors or reactors demand a thorough understanding of the hydrodynamic properties of the beds. Towards this end, pressure fluctuations in these beds have been extensively studied by numerous investigators [see, e.g., Fan et al., 1986; Zeng et al., 1988; Kang et al., 1992, 1999; Kwon et al., 1994; Chen et al., 1995; Pang and Kim, 2001].

In previous works, the behavior of fluidized beds and the quality of fluidization have been successfully studied by analyzing pressure fluctuations [Fan et al., 1981, 1986; Lee and Kim, 1988; Zeng et al., 1988; Hong et al., 1990; Kang et al., 1992; Kwon et al., 1994; Chen et al., 1995; Shen et al., 1995]. Fan et al. [1986] were the first to adopt this technique to study the pressure-fluctuation behavior in a three-phase fluidized bed; they have concluded that this technique might also be effective for studying flow regimes and that the power-spectral-density function is distinctly different for vari-

ous flow regimes. Zheng et al. [1988] studied the pressure-fluctuation signals in a three-phase fluidized bed of air, water, and glass beads and have found that the characteristics of the root mean square and the power-spectral-density function of these signals appreciably vary with the operating conditions and that the analysis of pressure fluctuations is effective for identifying flow regimes.

It has been pointed out that the formation, motion, break-up and coalescence of bubbles are the main causes of pressure fluctuations in fluidized beds [Fan et al., 1981]. While such pressure fluctuations have been extensively investigated, they are yet to be fully understood because of their highly random and stochastic nature.

This work is aimed at exploring in detail the hydrodynamic properties of bubbling flow through a three-phase fluidized bed with a moderately large diameter (0.376 m) in terms of pressure fluctuations. A comprehensive set of experimentally measured, pressure-fluctuation data was extensively analyzed statistically and stochastically.

EXPERIMENT

The materials and facilities are outlined. Subsequently, the procedure is described in some detail.

1. Materials

The fluidizing liquid and gas were water and oil-free compressed air, respectively. The fluidized solid comprised two groups of spherical glass beads, both with a density of 2,500 kg/m³. One group had a diameter of 1.0 mm (0.001 m); and the other, 2.3 mm (0.0023 m).

2. Facilities

The experimental facilities, shown in Fig. 1, consisted of an assembly of a three-phase-fluidized bed, a measuring assembly, and a calculating/recording assembly. All experiments were carried out in a Plexiglas column at room temperature (25±1 °C) under atmospheric pressure. The column's inside diameter was 0.376 m, and

[†]To whom correspondence should be addressed.

E-mail: drpark@woosuk.ac.kr

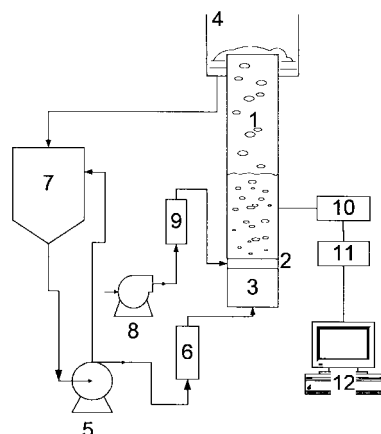


Fig. 1. Schematic diagram of experimental apparatus.

- | | |
|--------------------|-----------------------------|
| 1. Main column | 7. Liquid reservoir |
| 2. Distributor | 8. Air compressor |
| 3. Calming section | 9. Flowmeter |
| 4. Weir | 10. Pressure |
| 5. Pump | 11. Data acquisition system |
| 6. Flowmeter | 12. PC |

its height was 2.1 m. A perforated plate with 786 evenly spaced holes, 3 mm (0.003 m) in diameter, served as the liquid distributor. Air was fed to the column through a grid of feed pipes, each with an inside diameter of 6.4 mm; the grid was provided with 232 horizontally drilled holes, 1 mm in diameter. Pressure taps to measure the static pressure with a liquid manometer were mounted flush along the wall of the column; they were axially distributed, and the distance between any pair of adjacent taps was 0.14 m.

The pressure tap for measuring pressure fluctuations was located at 0.4 m above the distributor. One of the two channels of a differential pressure transducer was connected to this pressure tap. The differential pressure transducer generated an output voltage proportional to the pressure-fluctuation signal. The signal was stored in a data acquisition system (Data Precision Model, D-6000), and then the one was filtered by using a low pass filter (<60 Hz) and processed by a personal computer.

3. Procedure

In each experimental run, the particles were suspended in the bed by the fluidizing gas at a flow rate within the range between 0 and 0.10 m/s, and the fluidizing liquid at a flow rate within the range between 0 and 0.10 m/s. Once a steady state was reached, the fluctuating voltage-time signals, corresponding to the fluctuating pressure-time signals, from the differential pressure transducer were sampled at a rate of 0.01 s and stored in the data acquisition system. The overall data acquisition time was 41 s, thereby yielding a total of 4100 data points. The signals were transmitted to the computer. Statistical properties of the pressure fluctuations, including the mean, standard deviation, skewness, kurtosis, and the power-spectral-density function, were calculated from the digitized data acquired with the computer.

RESULTS AND DISCUSSION

An extensive set of pressure-fluctuation signals was recorded by varying the three major operational variables, i.e., the gas flow rate,

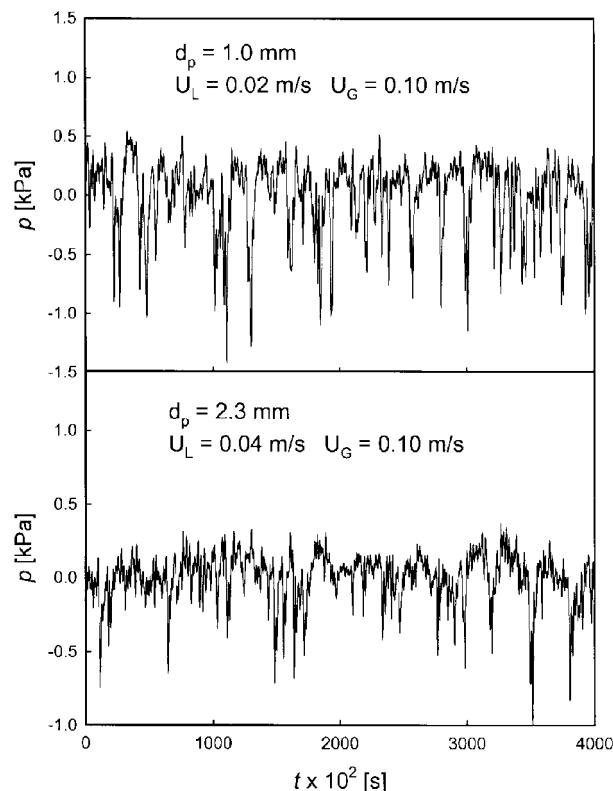


Fig. 2. Typical pressure-fluctuation signals.

the liquid flow rate, and the particle size. The gas flow rate ranged from 0 to 0.10 m/s; the liquid flow rate ranged from 0 to 10 m/s; and the particle sizes were 1 mm (0.001 m) and 2.3 mm (0.0023 m) in diameter. The typical pressure-fluctuation signals recorded, as illustrated in Fig. 2, have yielded the estimates of statistical parameters or summary statistics in terms of the histogram, standard deviation, skewness and kurtosis, and power-spectral-density function. The differences among the signals can be clearly discerned from these statistical parameters despite the similarity in appearance of the signals.

1. Histogram

Histograms have been generated for pressure fluctuations, (p' - \bar{p}), recorded under various sets of operating conditions. Each his-

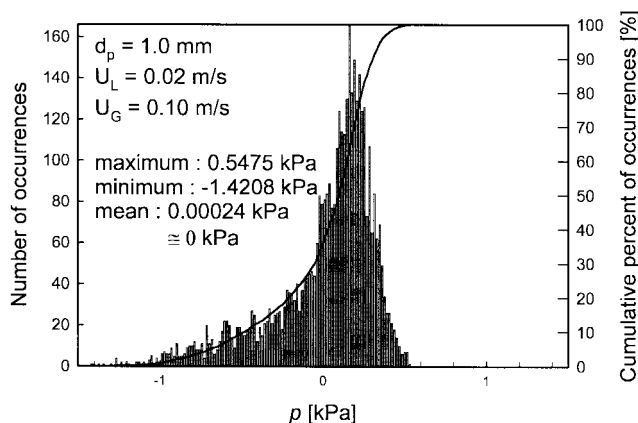


Fig. 3. Typical histogram of pressure fluctuations.

togram gives rise to the maximum and minimum as well as the mean of the distribution under a given set of operating conditions. A typical histogram of pressure fluctuations is shown in Fig. 3.

The random variable of concern in the present work, p' , the pressure fluctuations, is a specific value of which is denoted by p' as given in the experimental section. Theoretically, the mean value or the first moment of P' , i.e. \bar{p}' , given by

$$\bar{p}' = \int_{-\infty}^{\infty} p' f(p') dp' \quad (1)$$

is zero for a steady-state, stationary time series of pressure fluctuations. Nevertheless, for the digitally recorded or discrete data of this series, the sample mean computed by

$$\bar{p}' = \sum_{i=1}^I p'_i x_i \quad (2)$$

where i is a number of recorded digital data of pressure fluctuation signals and x_i is probability of the i th datum to occur, in usually a small value, slightly deviating from the theoretical value of 0, as noted in Fig. 3.

2. Maximum and Minimum

The maximum and minimum amplitudes of pressure fluctuations in three-phase fluidized beds containing particles of 1 mm (0.001 m) and 2.3 mm (0.0023 m) in diameter are presented as functions of the gas flow rate, U_G , in Fig. 4. The difference between the maximum and minimum amplitudes is magnified with the increase in U_G because bubbles are enlarged through coalescence [Kim et al., 1977; Han and Kim, 1993; Kim and Kang, 1996].

Fig. 5 illustrates the effects of the liquid flow rate, U_L , on the maximum and minimum amplitudes of pressure fluctuations. As U_L increases, the difference between the maximum and minimum is nar-

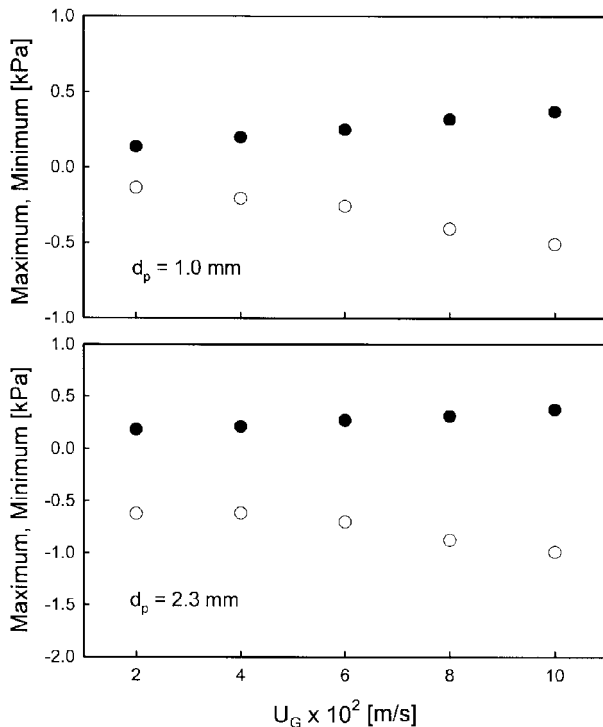


Fig. 4. Effect of the gas flow rate on the mean, maximum, and minimum ($d_p=1.0$ and 2.3 mm).

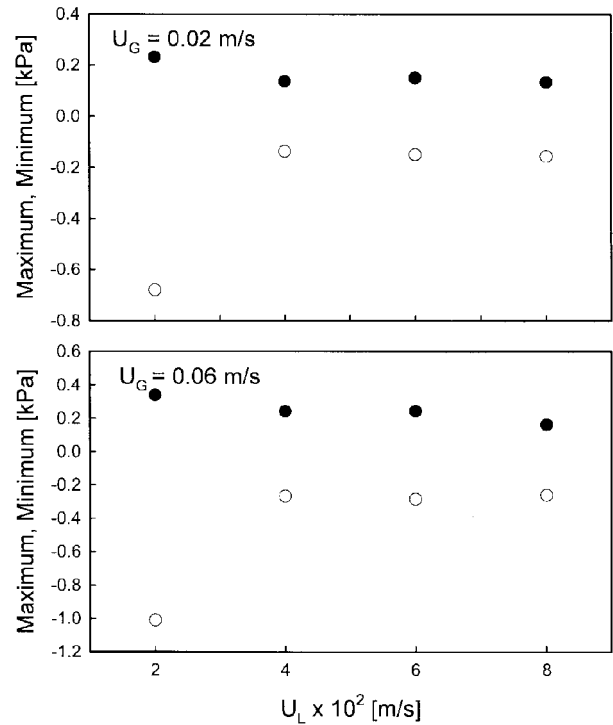


Fig. 5. Effect of the liquid flow rate on the mean, maximum, and minimum ($d_p=1.0$ mm).

rowed due to the breakage of larger bubbles by shear exerted on these bubbles by the flowing liquid.

The effects of the particle size, d_p , on the maximum and minimum amplitudes of pressure fluctuations can also be discerned in Fig. 4. The difference between the maximum and minimum amplitudes is broader for the larger particles than for the smaller ones, even though the patterns of such decreases are similar. It is known that the larger particles generate bigger bubbles than the smaller particles [Kwon et al., 1994]. Hence, the differences in the maximum and minimum amplitudes of pressure fluctuations are broadened as d_p increases.

3. Standard Deviation

The standard deviation of pressure fluctuations is the positive

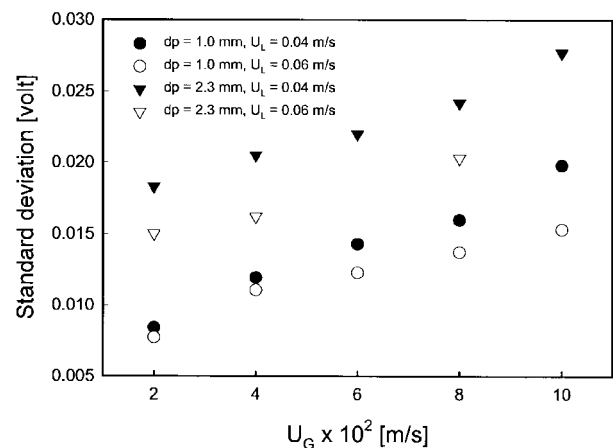


Fig. 6. Effect of the gas flow rate on the standard deviation.

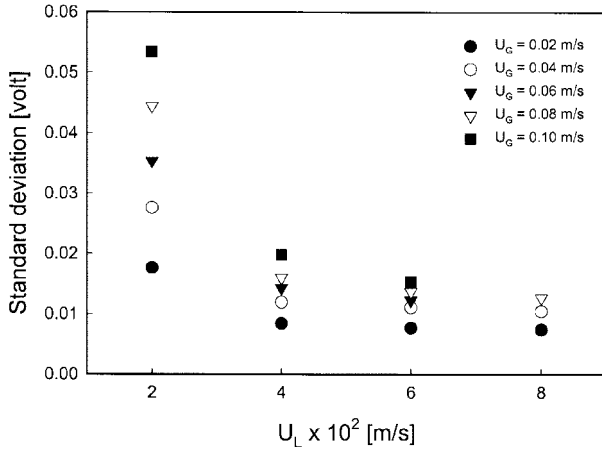


Fig. 7. Effect of the liquid flow rate on the standard deviation ($dp=1.0$ mm).

square root of the second central moment, i.e., the variance. Here, the standard deviation can be computed as

$$\sigma = [\int_{-\infty}^{\infty} (p' - \bar{p}')^2 dp']^{1/2} \quad (3)$$

where \bar{p}' are the mean of pressure fluctuations.

The standard deviations of pressure fluctuations, σ 's, are presented as functions of the gas flow rate, U_G , in Fig. 6. They increase with an increase in U_G ; this may be attributable to the expansion of bubbles due to the enhanced bubble coalescence with the increase in U_G . It has been reported that the bubble-coalescence regime exists in a fluidized bed of the air-water-glass beads system of the diameters of the beads are less than 0.00254 m [Kim et al., 1972, 1975; Kim and Kang, 1996].

The effect of the liquid flow rate, U_L , on the standard deviation of pressure fluctuations, σ , is illustrated in Fig. 7. As U_L increases, σ decreases: the increase in U_L intensifies the breakage of larger bubbles due to the enhanced shear.

The variation of the standard deviation, σ , with the particle size, d_p , can also be discerned in Fig. 6. The σ in the bed of the larger particles is greater than that in the bed of the smaller particles under the same operating conditions. This can be expected from the decrease in the difference between the maximum and minimum amplitudes of pressure fluctuations as indicated in Fig. 4.

4. Skewness

The third central moment, i.e., the skewness, S , is a measure of the lack of symmetry in the probability-density function about the mean. The S is defined as

$$S = \frac{1}{\sigma^3} \int_{-\infty}^{\infty} (p' - \bar{p}')^3 f(p') dp' \quad (4)$$

where p' is the fluctuating pressure; \bar{p}' , the mean of the pressure; σ , the standard deviation; and $f(p')$, the probability density function of p' ; the \bar{p}' is zero here. The effects of the gas flow rate, U_G , illustrated in Fig. 8, indicate that S decreases as U_G increases. As stated earlier, the greater U_G , the larger the bubble size, thereby causing the amplitude of pressure fluctuations to magnify. This, in turn, makes the probability-density function or histogram of pressure fluctuations to increasingly skew to the right.

Fig. 9 presents the effects of the liquid flow rate, U_L , on the skew-

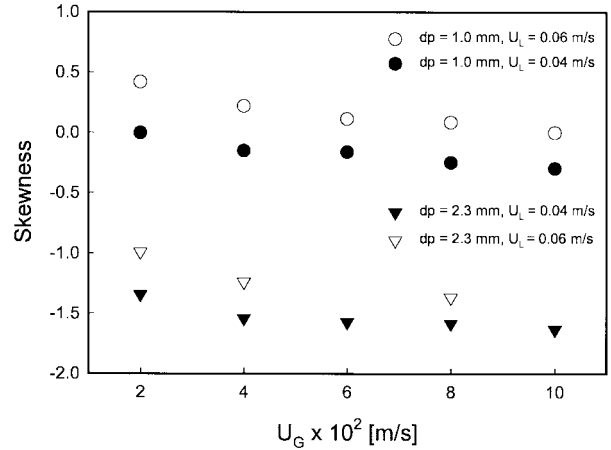


Fig. 8. Effect of the gas flow rate on the skewness.

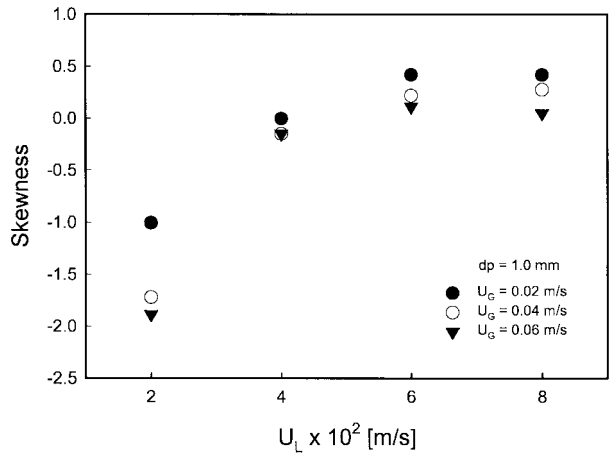


Fig. 9. Effect of the liquid flow rate on the skewness ($dp=1.0$ mm).

ness, S . As U_L increases, S of pressure fluctuations increases due to the enhanced breakup of the larger bubbles into the smaller ones.

In addition to the effects of the gas flow rate, U_G , Fig. 8 reveals the variation of the skewness, S , with the particle size, d_p . The S in the bed of larger particles is lower than that in the bed of smaller particles. It has been known that a bed with larger particles tends to contain more larger bubbles than a bed with smaller particles [Kwon et al., 1994]. As stated repeatedly, the larger bubbles cause the amplitude of pressure fluctuations to magnify. This makes the probability-density function skew to the right for the larger particles more than for the smaller particles.

5. Kurtosis

The fourth central moment or the kurtosis, K , is a measure of the extent of sharpness in probability-density function about the mean; the K is defined as

$$K = \frac{1}{\sigma^4} \int_{-\infty}^{\infty} (p' - \bar{p}')^4 f(p') dp' \quad (5)$$

The value of \bar{p}' is 0 in this work.

Fig. 10 exhibits the effects of the gas flow rate, U_G , on the kurtosis of pressure fluctuations, K ; note that K is nearly constant for the particles of either size at a given liquid flow rate, U_L . As U_L increases,

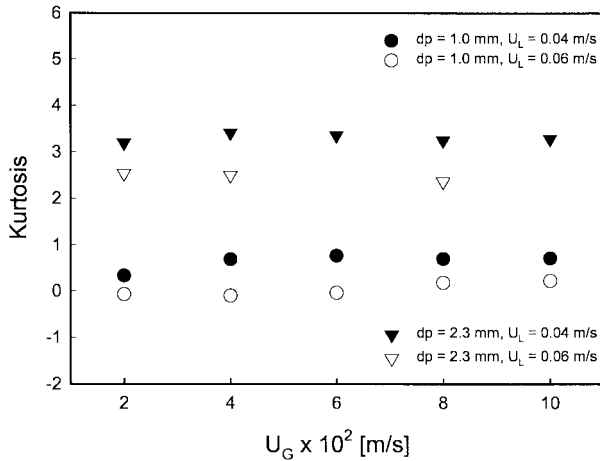


Fig. 10. Effect of the gas flow rate on the kurtosis.

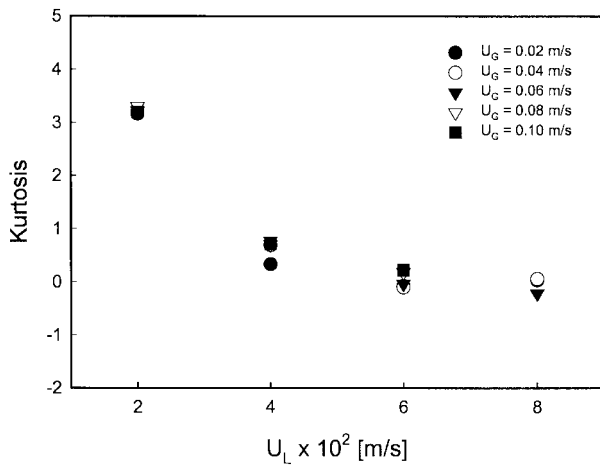


Fig. 11. Effect of the liquid flow rate on the kurtosis ($d_p=1.0$ mm).

however, K decreases sharply, thereby indicating that the distribution about the mean of pressure fluctuations is broadened appreciably; see Fig. 11. This is attributable to the breakup of the larger bubbles into the smaller bubbles due to shear exerted by the fluctuating flow of the fluidizing liquid.

The effect of the particle size, d_p , on the kurtosis, K , can also be observed in Fig. 10; the larger the d_p , the greater the K . This implies that the distribution about the mean of pressure fluctuations is flattened by the enlargement in the particle size. This is attributable to the breakup of the larger bubbles into the smaller bubbles due to the impact exerted by the fluidizing particle: the larger particle, the greater impact.

6. Power-Spectral-Density Function

The power-spectral-density functions of pressure fluctuations, $G_p(f)$'s, have been calculated and are presented in Figs. 12 and 13; the former illustrates the effects of the gas flow rate, U_G , and the latter, the effects of the liquid flow rate, U_L . The $G_p(f)$ is the Fourier transform of the auto-correlation function of pressure fluctuations, $R_p(\tau)$, i.e.,

$$G_p(f) = 2 \int_{-\infty}^{\infty} R_p(\tau) e^{-j2\pi f\tau} d\tau \quad (6)$$

where

$$R_p(\tau) = \lim_{T \rightarrow \infty} \frac{1}{T} \int_0^T p'(t)p'(t+\tau) dt$$

A peak or peaks in $G_p(f)$ correspond, respectively, to a major periodic component or components in the random variable. Thus $G_p(f)$ can show the intensity of corresponding objects, usually bubbles, in a sampling period. In the present work, $G_p(f)$ has been computed by the fast Fourier-transform method [Fan et al., 1981, 1983, 1986; Lee and Kim, 1988; Shen et al., 1995].

Note that in Fig. 12, a distinct peak appears between 0 and 2 Hz in the power-spectral-density function, $G_p(f)$. As the frequency, f , exceeds 20 Hz, $G_p(f)$ becomes negligible regardless of the gas flow rates, U_G . The greater the U_G , the broader the distribution of $G_p(f)$ and the higher the major frequency, apparently as a result of the

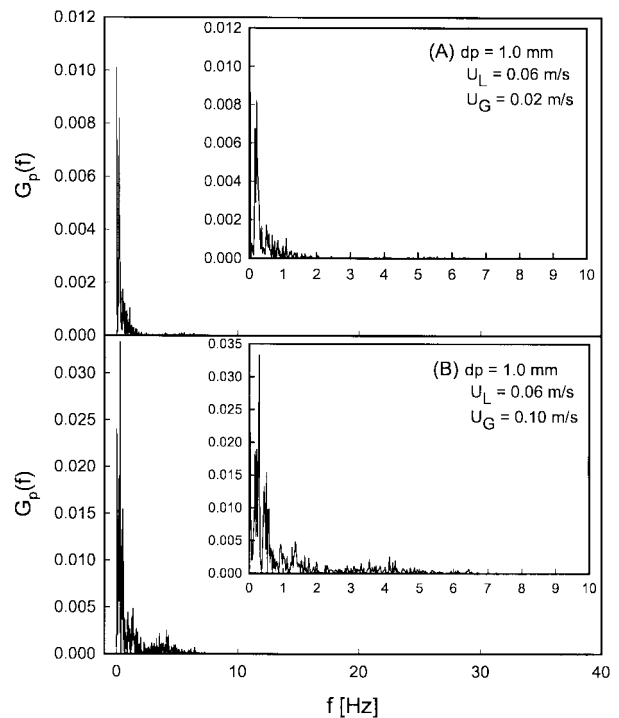


Fig. 12. Variation of the power-spectral-density function with the gas flow rate.

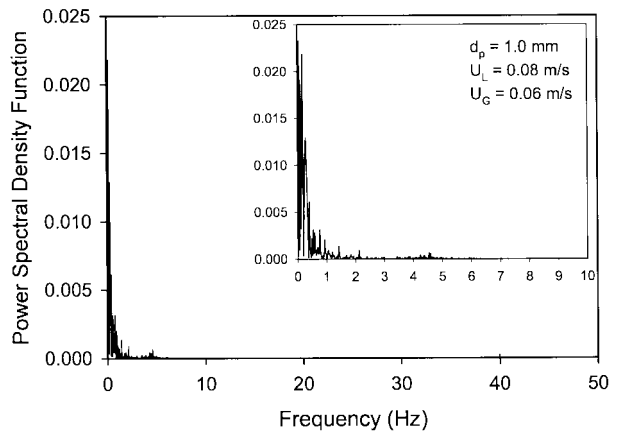


Fig. 13. Variation of the power-spectral-density function with the liquid flow rate.

bubble coalescence.

In contrast to Fig. 12, Fig. 13 shows that the greater the liquid flow rate, U_L , the narrower the distribution of the power-spectral-density function, $G_p(f)$, and the higher the major frequency. This is attributable to the break-up or dispersion of bubbles.

CONCLUSIONS

Experimentally measured pressure fluctuations in a three-phase fluidized bed with a moderately large diameter have been extensively characterized statistically and stochastically. This has yielded the fluctuations' histogram, maximum amplitude and minimum amplitude, difference between the maximum and minimum amplitudes, standard deviation, skewness, kurtosis, and power-spectral-density function.

As the gas flow rate increases, the difference between the maximum and minimum amplitudes broadens, the standard deviation increases, the skewness decreases, the distribution of the power-spectral-density function broadens, and the major frequency increases. All these variations are mainly attributable to the enhancement of bubble coalescence with the elevation in the gas flow rate. In contrast, as the liquid flow rate increases, the difference between the maximum and minimum amplitudes narrows, the standard deviation decreases, the skewness increases, the kurtosis increases, the power-spectral-density function narrows, and the major frequency diminishes. All these variations are mainly due to the enhanced disintegration of bubbles induced by intensified shear stress exerted by liquid flow.

The results of the present work unequivocally demonstrate that the hydrodynamic characteristics of bubbling flow through a three-phase fluidized bed with a moderately large diameter in terms of pressure fluctuations are strongly affected by the flow rates of both the fluidizing gas and liquid. The results also demonstrate that, without exception, the effects of these three variables on the estimates of various statistical properties or summary statistics of the pressure fluctuations can be consistently interpreted.

ACKNOWLEDGMENT

Authors wish to acknowledge the support of Woosuk University.

NOMENCLATURE

d_p : particle diameter [m]
 f : frequency [Hz]
 $f(p)$: probability density function
 $G_p(f)$: power-spectral-density function
 p : pressure fluctuations [Pa]
 \bar{p} : mean of pressure fluctuations [Pa]
 $R_p(\tau)$: autocorrelation function
 t : time [s]
 T : observation time [s]
 U_G : superficial gas flow rate [m/s]
 U_L : superficial liquid flow rate [m/s]

Subscripts

G : gas

L : liquid
 Max : maximum
 Min : minimum
 P : particle

REFERENCES

- Chen, Z., Zheng, C., Feng, Y. and Hofman, H., "Distributions of Flow Regimes and Phase Holdups in Three-Phase Fluidized Beds," *Chem. Eng. Sci.*, **50**, 2153 (1995).
 Epstein, N., "Three-Phase Fluidization: Some Knowledge Gaps," *Can. J. Chem. Eng.*, **59**, 649 (1981).
 Fan, L. S., "Gas-Liquid-Solid Fluidization Engineering," Butterworths, Boston (1989).
 Fan, L. S., Satija, S. and Wisecarver, K., "Pressure Fluctuation Measurements and Flow Regime Transitions in Gas-Liquid-Solid Fluidized Beds," *AIChE J.*, **32**, 338 (1986).
 Fan, L. T., Ho, T. C., Hiraoka, S. and Walawender, W. P., "Pressure Fluctuations in a Fluidized Bed," *AIChE J.*, **27**, 388 (1981).
 Fan, L. T., Ho, T. C. and Walawender, W. P., "Measurements of the Rise Velocities of Bubbles, Slugs and Pressure Waves in a Gas-Solid Fluidized Bed Using Pressure Fluctuation Signals," *AIChE J.*, **29**, 33 (1983).
 Han, J. H. and Kim, S. D., "Bubble Chord Length Distribution in Three-Phase Fluidized Beds," *Chem. Eng. Sci.*, **48**, 1033 (1993).
 Han, J. H., Wild, G. and Kim, S. D., "Phase Holdup Characteristics in Three Phase Fluidized Beds," *Chem. Eng. J.*, **43**, 67 (1990).
 Ho, T. C., Ko, K. N., Chang, C. C. and Fan, L. T., "Dynamic Simulation of a Shallow-Jetting Fluidized-Bed Coal Combustor," *Power Technology*, **53**, 247 (1987).
 Hong, S. C., Jo, B. R. and Doh, D. S., "Determination of Minimum Fluidization Velocity by the Statistical Analysis of Pressure Fluctuations in a Gas-Solid Fluidized Bed," *Powder Technology*, **60**, 215 (1990).
 Kang, Y., Min, B. T., Kim, S. D., Yashima, M. and Fan, L. T., "Stochastic Analysis of the Effects of Bubble-breakers on Pressure Fluctuations in a Three-Phase Fluidized Bed," Proceeding Twenty-Third Annual Meeting of the Fine Particle Society, Las Vegas, NV (1992).
 Kang, Y., Woo, K. J., Ko, M. H., Cho, Y. J. and Kim, S. D., "Particle Flow Behavior in Three-Phase Fluidized Beds," *Korean J. Chem. Eng.*, **16**, 784 (1999).
 Kim, J. O. and Kim, S. D., "Bubble Characteristics of Three Phase Fluidized Beds of Floating Bubble Breakers," *Particulate Sci. Technol.*, **5**, 309 (1987).
 Kim, S. D., Baker, C. G. J. and Bergougnou, M. A., "Holdup and Axial Mixing Characteristics of Two and Three Phase Fluidized Beds," *Can. J. Chem. Eng.*, **50**, 695 (1972).
 Kim, S. D., Baker, C. G. J. and Bergougnou, M. A., "Phase Holdup Characteristics of Three-Phase Fluidized Beds," *Can. J. Chem. Eng.*, **53**, 134 (1975).
 Kim, S. D., Baker, C. G. J. and Bergougnou, M. A., "Bubble Characteristics in Three-Phase Fluidized Beds," *Chem. Eng. Sci.*, **32**, 1299 (1977).
 Kim, S. D. and Kang, Y., "Dispersed Phase Characteristics in Three-Phase Fluidized Bed in Encyclopedia of Fluid Mechanics, Mixed-Flow Hydrodynamics-Advances in Engineering Fluid Mechanics Series," Chapter 37, 845 (1996).
 Kwon, H. W., Kang, Y., Kim, S. D., Yashima, M. and Fan, L. T., "Bub-

- ble-Chord Length and Pressure Fluctuations in Three-Phase Fluidized Beds," *Ind. Eng. Chem. Res.*, **33**, 1852 (1994).
- Lee, G. S. and Kim, S. D., "Pressure Fluctuations in Turbulent Fluidized Beds," *J. of Chem. Eng. of Japan*, **21**, 515 (1988).
- Park, S. H. and Kim, S. D., "Wavelet Transfer Analysis of Pressure Fluctuation Signals in a Three-Phase Fluidized Bed," *Korean J. Chem. Eng.*, **18**, 1015 (2001).
- Shah, Y. T., Kelka, B. G., Godbole, S. P. and Deckwer, W. D., "Design Parameters Estimations for Bubble Column Reactors," *AIChE J.*, **28**, 353 (1982).
- Shen, B. C., Fan, L. T. and Walawender, W. P., "Bulk-Density Distribution of Solids in the Freeboard of a Gas-Solid Fluidized Bed," *Ind. Eng. Chem. Res.*, **34**, 1919 (1995).
- Zeng, C., Yao, B. and Feng, Y., "Flow Regime Identification and Gas Hold-up of Three-phase Fluidized Systems," *Chem. Eng. Sci.*, **43**, 2195 (1988).